academicJournals

Vol. 10(11), pp. 359-363, 16 June, 2015
DOI: 10.5897/IJPS2015.4358
Article Number: A96694253649
ISSN 1992 - 1950

http://www.academicjournals.org/IJPS

International Journal of Physical Sciences

Full Length Research Paper

Microwave propagation attenuation due to earth's atmosphere at very high frequency (VHF) and ultra-high frequency (UHF) bands in Nsukka under a clear –air condition

Ernest Benjamin Ikechukwu Ugwu[1,2]*, Maureen Chioma Umeh[1] and Obiageli Josephine Ugonabo[1]

[1]Department of Physics and Astronomy, University of Nigeria, Nsukka, Enugu State, Nigeria.
[2]Natural Science Unit, University of Nigeria, Nsukka, Enugu State, Nigeria.

Received 26 April, 2015; Accepted 1June, 2015

The microwave propagation attenuation due to earth's atmosphere under a clear-air condition for fade depth of 10 dB was investigated using refractivity data calculated from weather vagaries measurement carried out between January and December 2008. The International Telecommunication Union-Radiocommunication Sector (ITU-R) model for multipath fading for small percentage of time with link distance of 100 km was used. The result showed that at this distance, the refractivity gradient has a strong correlation of 0.747 with percentage of time that the fade depth was exceeded. It was also observed that the percentage of time that the fade depth was exceeded increases with frequency until about 1.2GHz when the result becomes unreliable.

Key words: Attenuation, fade depth, microwave, multipath fading, refractivity gradient.

INTRODUCTION

The meteorological effect on microwave signals especially at very high frequency (VHF) and ultra-high frequency (UHF) band is very significant. Several clear-air effects (Oyedum, 2007), such as, sub-refraction, super-refraction, ducting and scattering due to variations in tropospheric condition can seriously enhance or degrade the quality of reception of a microwave communication link (Ayantunji and Okeke, 2011; Falodun and Okeke, 2013).

There are several sources of signal attenuations that can affect a microwave signal in the troposphere. These attenuations include beam spreading (defocusing), antenna decoupling, atmospheric gaseous absorption, rain attenuation, tropospheric scattering under a clear-air-condition, and multipath fading among others. Most of these mechanisms can occur by themselves or in combination with each other (ITU-R P.530-8).

Multipath fading is the most common type of fading encountered, particularly on line-of-sight (LOS) radio links. It is the principal cause of dispersion, which is particularly troublesome on digital troposcatter and high-bit-rate LOS links. For an explanation of atmospheric

*Corresponding author. E-mail: ernestb.ugwu@unn.edu.ng, Tel: +2348066953787.

multipath fading, we must turn to the refractive index gradient. As the gradient varies, multipath fading results, owing to the:

1. Interference between direct rays and the specula component of a ground-reflected wave;
2. The non-specula component of the ground-reflected wave;
3. Partial reflections from atmospheric sheets or elevated layers;
4. Additional direct wave paths and non-reflected paths.

One or more of these multipath fading mechanisms may occur at a time. Of interest to the radio link design engineer is the fading rate (the number of fades per unit time) and the fading depth (the magnitude of the variation of the signal intensity at the receiver from its free-space value expressed in decibels).

Fade depths can exceed 20 dB, particularly on longer LOS paths and more than 30 dB on longer troposcatter paths (Freeman, 2007; Grabner et al., 2011). Fade durations of up to several minutes or more can be expected. Often multipath fading is frequency selective and the best technique for mitigation is frequency diversity. For effective operation of frequency diversity, sufficient frequency separation is required between the two transmit frequencies to provide sufficient de-correlation.

Rain intensity, refractivity gradient and annual mean temperature are critical parameters affecting link performance (Agba et al., 2011). Fades due to atmospheric multipath are very important, particularly for point-to-point microwave links. The effect occurs predominantly in higher-humid areas during night time hours, with coastal areas being particularly susceptible (Seybold, 2007). Like refraction, atmospheric multipath only affects paths that are very nearly horizontal. Atmospheric multipath is primarily observed over very flat terrain; irregular terrain makes formation of a uniform atmospheric layer unlikely. The impact of this kind of multipath on terrestrial point-to-point microwave links was studied by Bell Laboratories in the 1960s and 1970s. Models (Morita model, 1970 used in Japan, Barnett-Vigants models, 1970 and 1972 widely used in the United States and Segal model, 1992 used in Canada, ITU-R models used worldwide) were developed for predicting the multipath distribution effects on terrestrial LOS links (Agba et al., 2011). The ITU-R model is periodically updated. An evaluation of the prediction equation for the revised and previous ITU-R models and other regional models like Barnett-Vigants and Morita models showed that the revised ITU model (2001) slightly performed better than the other models for both overland and coastal/overwater links (Olsen et al., 2003). The revised ITU model (2001) is adopted in this work.

The ITU model for atmospheric multipath has two different formulations for low probability of fade and another formulation for all fade probabilities. For most applications, the low fade probability is apt. In addition to providing multipath fade depth predictions, the ITU model also provides a model for multipath signal enhancement. The enhancement model is not presented herein, but it may be of interest in assessing the potential for interference in frequency re-use application.

The available data for multipath fading is usually based on data from coastal areas because the effect occurs predominantly in higher humid region. This might not be entirely true since tropospheric refractive index has a distinct dependence on weather vagaries (air temperature, air pressure and relative humidity) in Nsukka, Nigeria (Ayantunji and Umeh, 2010). Spatial distribution of the refractive index of the air, especially its vertical profiles, affects the propagation of electromagnetic waves in atmosphere (Grabner et al., 2013). In the hinterland areas with large concentration, it is important that the effect of multipath on radio frequency propagation be carried out to enhance the communication system.

METHODOLOGY AND INSTRUMENTATION

The Centre for Basic Space Science (CBSS), University of Nigeria, Nsukka, Nigeria provided the data for determining the radio refractivity gradient. The CBSS has Vantage Pro2 automatic weather stations installed on Nigeria Telecommunication (NITEL) mast at the ground level (0m height) and at 100 m height that collect data every 30 s via the integrated sensor suite (ISS) and the data are transmitted to the console at 860 MHz. A GPS was used to determine the altitude of the site. Other data used were hypothetical and this was achieved by keeping some variables (like frequency, heights of the antennas, path separation, and fade depth) in the ITU model (2001) constant while one is varied.

For a clear-air condition (that is, atmosphere without rain, snow, fog or other conditions) radio refractivity expressed by equation (1) was computed for various months having calculated e_s and e using Equations (3) and (2) respectively.

The gradient of refractivity (dN) was calculated from the computation done for all values on the surface (0m) and at a height of 100 m above the surface level.

Tropospheric radio refractivity, N, and partial vapour pressure, e, are defined by the ITU-R (2003) formula in equations 1 and 2 respectively:

$$N = \frac{77.6P}{T} + 3.73 \times 10^5 \frac{e}{T^2} \quad (1)$$

$$e = R_h e_s / 100 \quad (2)$$

Where P is atmospheric pressure (hPa), T is temperature (K), R_h is relative humidity (%) and e_s is saturated vapour pressure (hPa) at a given temperature, t (°C) and is obtained from:

$$e_s = 6.112 exp\, 17.5t/(t + 240.97) \quad (3)$$

For a clear-air condition (that is, atmosphere without rain, snow, fog or other conditions) radio refractivity expressed by Equation (1) was computed for various months after calculating e_s and *e*. The gradient of refractivity (dN) was calculated from the computation

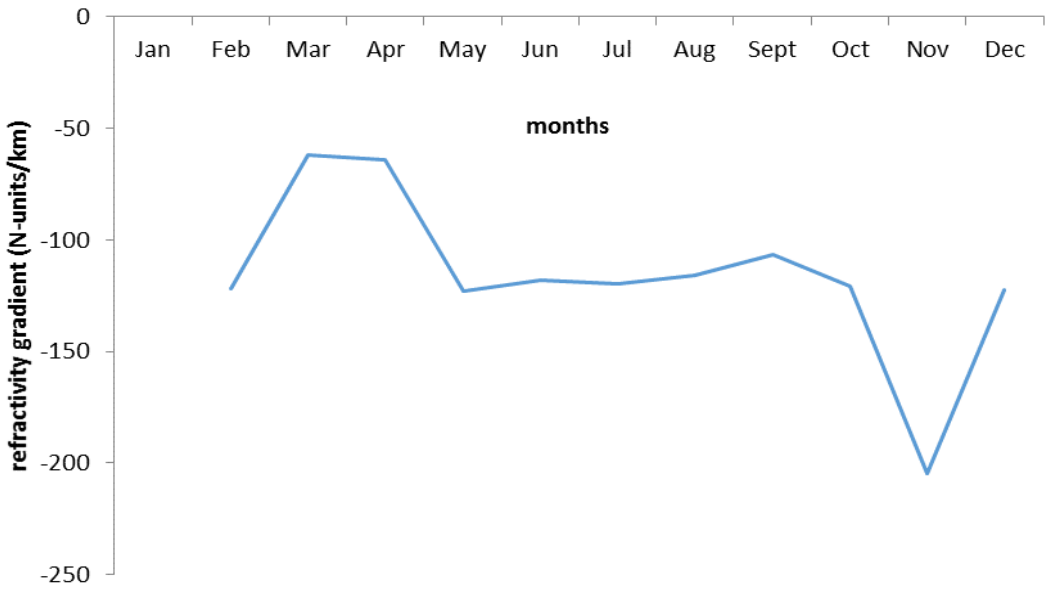

Figure 1. Seasonal variation of refractivity gradient.

done for all values on the surface (0 m) and at a height of 100 m above the surface level.

The first step in applying the ITU-R, 2001 for small percentages is to determine geoclimatic factor, K given by:

$$K = 10^{-3.9-0.003dN_1} s_a^{-0.42} \quad (4)$$

where dN_1 is the point refractivity gradient in the lowest 65m of the atmosphere not exceeded for 1% of an average year, and s_a is the area terrain roughness defined as the standard deviation of terrain heights (m) within a 110 km × 110 km area with a 30 s resolution (e.g. the Globe "gtopo30" data). The area was aligned with the longitude such that the two equal halves of the area are on each side of the longitude that goes through the path centre. The geoclimatic factor, K was determined using equation 5 since s_a is not available for Nsukka.

$$K = 10^{-4.2-0.0029dN_1} \quad (5)$$

The second step is to determine the magnitude of the path inclination, $|\varepsilon_p|$ given by:

$$|\varepsilon_p| = (|h_r - h_s|)/d \quad (6)$$

where $|\varepsilon_p|$ is the path inclination (mrad), h_r and h_s are the heights (in metres above sea-level or some other reference height) of the receiving and transmitting antenna respectively and d is the link distance, taht is, the separation between the two antennas (km).

For detailed link design, the percentage time or "worst month" outage probability, P_w for which a particular fade depth A (dB) is exceeded is given by:

$$P_w = Kd^{3.2}(1+|\varepsilon_p|)^{-0.97} \times 10^{0.032f-0.00085h_L-A/10}\ \% \quad (7)$$

where d is the path length (km), f is the frequency (GHz), h_L is the altitude of the lower antenna (m), and A is the fade depth (dB). P_w is expressed in % or seconds.

For quick design however, we used Equation (8):

$$P_w = Kd^{3.0}(1+|\varepsilon_p|)^{-1.2} \times 10^{0.033f-0.001h_L-A/10}\ \% \quad (8)$$

The path inclination, $|\varepsilon_p|$ and percentage time, P_w of attenuation for detailed design for which a particular fade depth is said to be exceeded were also computed. To calculate these, the following values were assumed; h_r = 20m; h_e = 150 m; d = 100 km (100,000 m); f = 1 GHz (1000 MHz); h_L = 20 m; A = 10 dB/m. Due to the large values, excel was used for these calculations.

RESULTS AND DISCUSSION

Figure 1 shows seasonal variation of refractivity gradient which maintains almost a constant value in the rainy season. This pattern of variation is probably due to the high humidity during the rainy season. The refractivity gradient peaked in the month of March which is an indication of the peak of dry season at Nsukka and decreases gradually in subsequent months of the year. Grabner et al. (2012) observed the largest values of refractivity index structure constant in the summer months and the least values in the winter months in Czech Republic. This indicates that the radio refractivity values vary with climatic zones as well as with the seasons of the year (Falodun and Okeke, 2013).

Figure 2 shows variation of percentage of time of attenuation with refractive gradient at 10 dB fade depth averaged over each month. From this we can deduce that the more negative the refractivity gradient the more

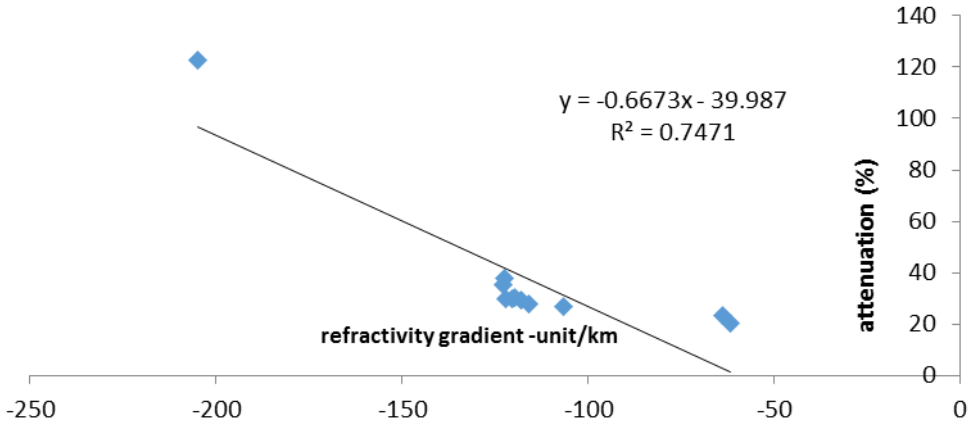

Figure 2. Variation of percentage of time for attenuation with refractivity gradient at 10 dB fade depth.

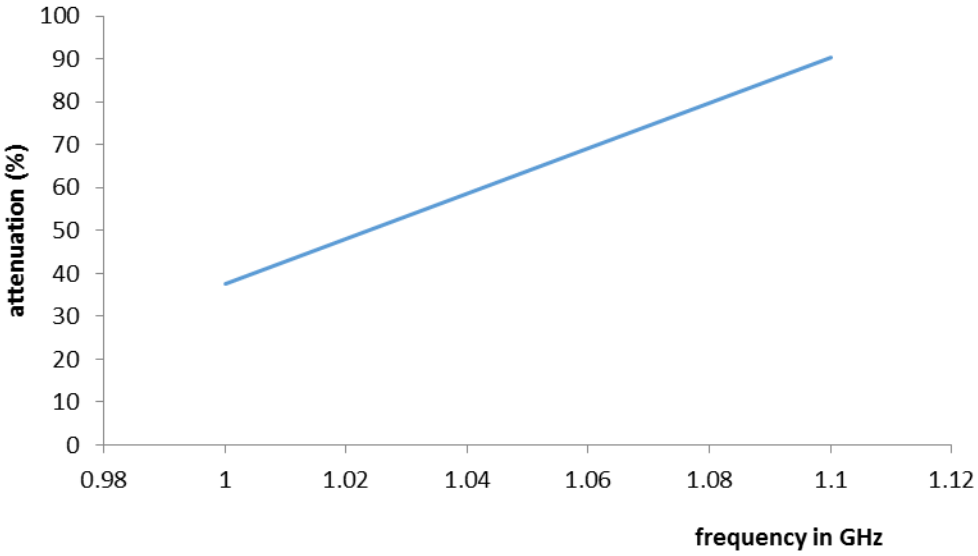

Figure 3. Variation of attenuation with frequency.

the attenuation. This implies lesser refractivity gradient and greater attenuation. The relationship:

$$P = -0.667dN - 39.98 \quad (9)$$

gives the relationship between percentage of time and refractivity gradient as obtained from the graph. A regression coefficient R^2 = 0.747 was obtained between the two variables. This shows high correlation.

Figure 3 shows variation of attenuation with frequency which was obtained from simulated data given in Table 1. This was obtained by varying the frequency using Equation (8) while other parameters remained constant. This shows that as frequency of transmission increases the attenuation increases. At frequencies greater than 1.2 GHz attenuation tends to infinity, which suggests that the study under clear-air condition is of little or no importance above this frequency. Under a clear-air condition, attenuation is proportional to frequency at VHF and UHF

Table 1. Variation of attenuation with frequency.

Frequency (GHz)	Attenuation due to clear-air condition (%)
1.0	37.59
1.02	48.18
1.04	58.76
1.06	69.34
1.08	79.90
1.10	90.51

bands and in line sections and low-loss adapters add significant contributions to the uncertainty of power measurements when the calorimeter correction factor is determined (Xiaohai and Crowley, 2011). An attempt was made to study the effects of variation of antennas' heights and the link distance at fade depth and frequency. No reasonable effect was observed.

We shall subsequently attempt to study in detail the effects of variation of the antenna height and the link distance at the fade depth and the frequency.

Conclusion

The results obtained from the study of microwave propagation attenuation due to earth's atmosphere under a clear-air condition for a fade depth of 10 dB suggest that refractivity gradient and percentage of time of attenuation at Nsukka have a very strong correlation of 0.747. This agrees with the results obtained by Westwater et al. (1990) in which there were a strong agreement between measurements and calculations with the least correlation at 0.9. They also observed that attenuation distributions are dependent on location and season

Also, the percentage of time of attenuation increases with increase in frequency unto about 1.2 GHz when the result becomes unreliable. Grabner et al. (2013) tried to model multipath propagation conditions but had unsatisfactory results. Horizontal spatial distribution of refractivity can be complex (Barrios, 1992), hence vertical refractivity profiles are not enough to describe propagation path under multipath conditions. The results obtained may improve radio communication system in Nigeria since only 25.82% of the entire land mass of Niger state, for example, has television signal coverage (Ajewole et al., 2013).

Conflict of Interest

The authors have not declared any conflict of interest.

REFERENCES

Agba BL, Ben-Sik-Ali O, Morin R, Bergeron G (2011). Recent evolution of ITU method for prediction of multipath fading on terrestrial microwave links. Progress in Electromagnetics Res. Symposium Proc. Marrakesh, Morocco, Mar. 20-23:1375.

Ajewole MO, Oyedum OD, Adediji AT, Moses AS, Eiche JO (2013). Spatial variability of VHF/UHF electric field strength in Niger State, Nigeria. Int. J. Digital Info. Wireless Comm. (IJDIWC) 3(3):231-239. The Society of Digital Information and Wireless Communications, 2013 (ISSN: 2225-658X).

Ayantunji BG, Okeke PN (2011) Diurnal and seasonal variation of surface refractivity over Nigeria. Progress in Electromagnetic Res. B. 30:201-222.

Ayantunji BG, Umeh MC (2010). Statistical study of the dependence of tropospheric refractive index on different weather vagaries. AFRICON2013. IEEE2013:133-180.

Barnett WT (1972). Multipath propagation at 4, 6, and 11GHz. The Bell Syst. Technol. J. 51(2):311-361.

Barrios A (1992). Parabolic equation modelling in horizontally inhomogeneous environments. IEEE Trans. Antennas Propagat. 40(7):791-797.

Falodun SE, Okeke PN (2013). Radiowave propagation measurements in Nigeria (preliminary reports). Theor. Appl. Climatol. 113:127–135. DOI 10.1007/s00704-012-0766-z.

Freeman RL (2007). Radio system design for telecommunication, Wiley Series in Telecomm. and Signal Processing. Wiley Interscience. John Willey and Sons, Inc.

Grabner M, Kvicera V, Pechac P (2011). First and second order statistics of clear-air attenuation on 11GHz terrestrial path. 6th European conference on antennas and propagation (EUCAP). IEEE: pp. 2401-2404.

Grabner M, Kvicera V, Pechac P, Jicha O (2012). Vertical dependence of refractive Index structure constant inlLowest troposphere. IEEE Antennas Wireless Propagat. Lett. 10:1473.

Grabner M, Kvicera V, Pechac P, Valtr P, Jicha O (2013). Atmospheric refractivity profiles and microwave propagation on a terrestrial path – experiment and simulation. 13th Conference on Microwave Techniques COMITE 2013, April 17-18, Pardubice, Czech Republic.

International Telecommunication Union (ITU-R, 2001). Propagation data and prediction methods required for the design of terrestrial line of sight systems. ITU, Geneva. pp. 530-539.

International Telecommunication Union (ITU-R, 2003). Propagation data and prediction methods required for the design of terrestrial line of sight systems. ITU, Geneva. pp. 530-538.

Morita K (1970). Prediction of Rayleigh fading occurrence probability of line of sight microwave links. Rev. Elec. Comm. Lab.18:310-321.

Olsen RL, Tjelta T, Martins L, Segal B (2003). Worldwide techniques for fading distribution on terrestrial L.O.S Links: Comparison with regional techniques. IEEE Trans. Antennas Propagation. 51(1):23-30.

Seybold JS (2007). Introduction to RF propagation. Wiley Interscience. John Willey and Sons, Inc.: pp. 116-118.

Westwater ER, Snider JB, Falls MJ (1990). Ground-based radiometric observations of atmospheric emission and attenuation at 20.6, 31.65, and 90.0GHz: A comparison of measurements and theory. IEEE trans. Antennas propagation. 38(10):1569-1579.

Oyedum OD (2007). Effects of tropospheric conditions on microwave propagation in Nigeria. Nig. J. Space Res. (NJSR). 3:81-100.

Xiaohai C, Crowley TP (2011). Comparison of experimental techniques for evaluating the correction factor of a rectangular waveguide microcalorimeter. IEEE Trans. Instrum. Meas. 60(7):2690-2695.